Michigan State University

National Superconducting Cyclotron Laboratory

# NEUTRON PRODUCTION IN HEAVY ION REACTIONS AT 35 AND 50 MeV/NUCLEON

H.R. SCHELIN, A. GALONSKY, C.K. GELBKE, H. HAMA, L. HEILBRONN, D. KROFCHECK, W.G. LYNCH, D. SACKETT, M.B. TSANG, X. YANG, F. DEAK, A. HORVATH, A. KISS, Z. SERES, J. KASAGI, and T. MURAKAMI

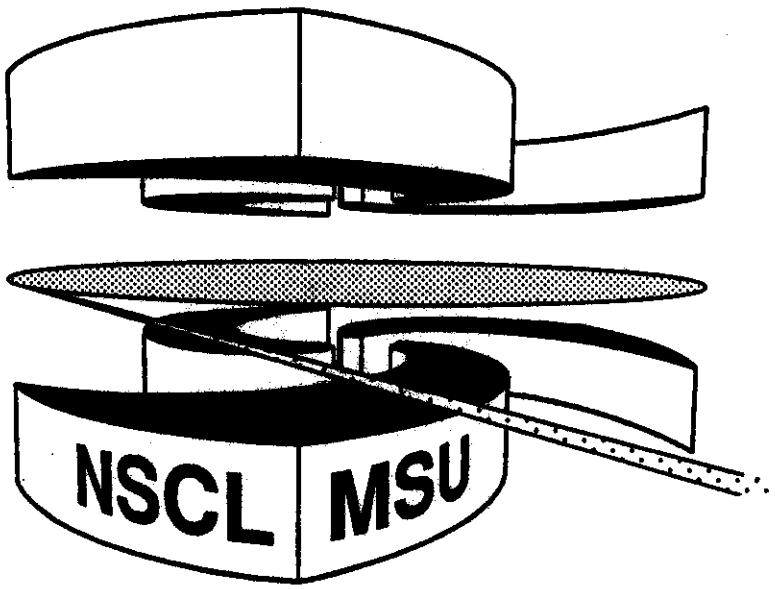


MSUCL-846 JUNE 1992

MSUCL-846
June, 1992

# Neutron Production in Heavy Ion Reactions at 35 and 50 MeV/nucleon

H.R. Schelin

Centro Tecnico Aeroespacial, Instituto de Estudos Avancados, Divisao de Fisica Teorica, C. P. 6044, CEP 12231, Sao Jose dos Campos, SP, Brazil

A. Galonsky, C.K. Gelbke, H. Hama,[Φ] L. Heilbronn,[†] D. Krofcheck,[*] W.G. Lynch, D. Sackett, M.B. Tsang, and X. Yang[α]

National Superconducting Cyclotron Laboratory and Department of Physics and Astronomy, Michigan State University, E. Lansing, Michigan 48824

F. Deák, A. Horvath, and A. Kiss

Department of Atomic Physics, Eötvös University, Budapest 114, Hungary H-1088

Z. Seres

Hungarian Academy of Sciences, Central Research Institute for Physics, Budapest 114, Hungary H-1525

J. Kasagi

Department of Physics, Tokyo Institute of Technology, O-Okayama, Meguro-Ku, Tokyo, Japan

and

T. Murakami

Department of Physics, Kyoto University, Kitasherakawa, Kyoto 606, Japan

---

To be published in Nuclear Science & Engineering

Abstract--Neutron spectra were measured by the time-of-flight method at laboratory angles from 15' to 120' for the reaction Ag(''N,n) at 50 MeV/nucleon. All spectra were fitted with a moving-source model. The cross section dependences on bombarding energy and on projectile mass were investigated by comparison with published neutron data from the reactions Ag(''N,n) at 35 MeV/nucleon and Ag(''Ar,n) at 35 MeV/nucleon. Application to biological hazard estimation is anticipated.

## I. INTRODUCTION

The use of heavy ion beams in science and technology has increased in recent years. Perhaps the most common use is in biomedical research. Amongst the heavy ion accelerators in operation for cancer treatment are the BEVALAC in Berkeley, California, the Schwerionensynchrotron in Darmstadt, Germany, and the Takahashi Radiation Chemistry Research Establishment in Japan.[1]

The radiation produced by heavy ion beams must be shielded for the safety of personnel and sometimes for the safety of special equipment. Since neutrons are the most penetrating radiation, the thicknesses of shielding walls depend on the energies and fluxes of neutrons resulting from the nuclear reactions of the heavy ions. It is therefore necessary to know the neutron production cross sections in order to calculate the shielding. In contrast to proton, deuteron, and alpha particle beams, neutron data from beams of heavier ions are still scarce.

The fragmentation of high-energy, high-Z particles (HZE) that are present in the galactic cosmic radiation field makes a significant contribution to the overall radiation dose received by astronauts engaged in long term missions outside the earth's magnetosphere.[2] The quality factor for neutrons has been estimated[2] to be in the range of 10 to 20. Because of this high value, the flux of neutrons may be a major component of the dose received from the fragmentation of HZE particles. Since only a little data[3-5] exists on the flux of neutrons from HZE fragmentation, the data presented here can be of some use to people assessing the overall radiation risk to astronauts on long-term missions.

We report here on a measurement of cross sections of neutrons emitted in the reaction $^{14}N$ + Ag at 50 MeV/nucleon. In two previous papers[6,7] we reported on similar neutron production cross sections in the reactions $^{14}N$ + Ag and $^{36}Ar$ + Ag at 35 MeV/nucleon. Combining the present results with the earlier results, we can now investigate the cross section dependence on bombarding energy (35 and 50 MeV/nucleon) as well as on projectile mass (A = 14 and 36).

## II. EXPERIMENTAL PROCEDURE

Since the apparatus and techniques used in the measurements are similar to those described elsewhere (Refs. 6 and 7 and references therein), we give but a brief description here. The K500 cyclotron at Michigan State University provided a $^{14}N$ beam at 50 MeV per nucleon. A schematic view of the experimental setup is shown in Fig. 1 of Ref. 7. The neutrons were detected with liquid scintillators (NE213 or BICRON501) placed at angles of 15°, 30°, 45°, 60°, and 120° relative to the incident beam direction. The detectors were positioned at distances ranging from 160 to 450 cm. Their intrinsic time resolution was about 0.8 ns. The neutrons were timed against the cyclotron rf signal and distinguished from gamma rays by a pulse shape discrimination scheme[8] using two commercial charge-integrating ADC's (QDC's). Detector efficiency was computed using a Monte Carlo code,[9] and attenuation of the neutrons by material lying

between the target and the detector was taken into account. In front of each detector was a 6-mm-thick NE102A veto paddle which rejected protons. The in-beam background contributions were measured by taking data with shadow bars between the target and the neutron detectors.

For each event we had the following information: detector number, a QDC signal proportional to total light output, a second QDC signal proportional to the light in the tail of the pulse, and a time signal relative to the cyclotron rf. The two QDC signals were used for neutron/$\gamma$-ray pulse-shape discrimination. Time-of-flight spectra for neutrons and gamma-rays were constructed off-line. After background subtraction, the neutron time spectra were converted to kinetic energy spectra with the flight time of the target $\gamma$-rays used as an absolute reference.

## III. EXPERIMENTAL RESULTS

Figure 1 shows the resulting energy spectra in the form of absolute double differential cross sections at five angles. These spectra exhibit exponential slopes that become steeper at the larger angles. It was shown[10] that such spectra can be described in terms of moving thermal sources. Three sources were adequate in the earlier work[7,8] and three are adequate here too.

The low-energy parts of the spectra, which have only a slight forward enhancement, can be attributed to a slowly-moving, target-like source -- Source #1, while the higher-energy parts, which have a more pronounced forward enhancement, are attributed to a more rapidly-moving source -- Source #2. A third source, #3, moves at a velocity only slightly below the beam velocity and contributes significantly only at small angles. Its presence can be seen in the broad bump centered around 40 MeV in the 15° spectrum. This source may be physically associated with neutron-emitting excited fragments created in peripheral collisions. The early result of more direct collisions, in which individual nucleons of the projectile strike nucleons of the target, is the generally forward emission of high energy neutrons. Source #2 represents this process. As the reaction proceeds, part of the projectile kinetic energy becomes thoroughly mixed into the heavy target nucleus forming Source #1, a slowly-moving compound nucleus.

The spectrum of neutrons from each source is isotropic in its own rest frame and has the Maxwellian form $\sqrt{E}\ E^{-E/T}$. In the laboratory, the complete distribution with respect to energy and angle is given by[10]

$$\frac{d^2\sigma}{dE\,d\Omega} = \sum_{i=1}^{3} \frac{N_i\sqrt{E/\pi}}{2\pi T_i^{3/2}} \times \exp\left[-\left|\frac{E - 2\sqrt{\varepsilon_i E}\cos\theta + \varepsilon_i}{T_i}\right|\right]. \qquad (1)$$

The data were fitted with this function using a chi-square minimization procedure. The source parameters $N_i$ (normalization factor, identified with the total cross section), $T_i$ (temperature or slope parameter) and $\varepsilon_i$ (source

velocity, actually $v_i^2/2$) were used as free parameters. The best fit to the experimental data is shown by the solid lines in Fig. 1, and the best-fit parameter values are listed in Table I. Parameter values for the two other projectiles, $^{14}N$ at 35 MeV/nucleon (Ref. 6) and $^{36}Ar$ at 35 MeV/nucleon (Ref. 7), are included in the table.

## IV. INTEGRATED CROSS SECTIONS

Two major benefits from the above fitting are the ease of extending the measured information into new regions of neutron energy or angle and the ease of integrating over each of these variables to give results in more digestible forms. Figures 2 and 3 show these integrals, Fig. 2 over neutron angle, leaving the absolute energy spectrum, and Fig. 3 over neutron energy, leaving the absolute angular distribution. The solid lines represent the data from the present work, the dashed lines the data from the $^{14}N$ + Ag reaction at 35 MeV/nucleon, and the dotted lines the data from the $^{36}Ar$ + Ag reaction at 35 MeV/nucleon.

In each figure there are relatively small differences amongst the three curves. For the reactions at the same projectile velocity, *i.e.*, the two at E/A = 35 MeV, the curves have almost the same shape in each figure. The magnitudes are greater for $^{36}Ar$, which has both more mass and, therefore, more kinetic energy, than $^{14}N$, and also more neutrons. As one might expect, the spectra (Fig.2) for the two experiments with a $^{14}N$ beam have more high energy neutrons with E/A = 50 MeV than with E/A = 35 MeV. Likewise, at the higher velocity of the 50-MeV experiment, Fig. 3 shows a more forward-peaked angular distribution than at the velocity of the 35-MeV experiment.

Another benefit is in estimating neutron yields from projectiles with mass numbers other than 14 or 36 and with energies other than 35 or 50 MeV/nucleon. That job is easier to accomplish with the values of source parameters in Table I than with the the measured spectral values themselves. Of course, with only three reactions, the table should be viewed as just a start.

## V. CONCLUSIONS

One may conclude that at 35 MeV/nucleon there are no drastic differences in neutron production with projectiles in the mass range 14 to 36. This covers a great range of heavy-ion projectiles, and undoubtedly, one could extrapolate to production with $^{12}C$, for example, with little error. On the other hand, in going from 35 MeV/nucleon to 50 MeV/nucleon, both the number and the forward concentration of high energy neutrons increases with projectile velocity. These increases could make a significant difference in the planning of radiation shielding against neutrons produced in heavy ion collisions.

It would be useful to measure neutron spectra with the same target and projectiles over a greater range of projectile energy, particularly at higher energies, so that the systematics of neutron production could be more clearly defined. This would be possible for example at the NSCL where the K-1200 cyclotron can provide beams of $^{14}N$ and $^{36}Ar$ up to 150 MeV/nucleon.

**ACKNOWLEDGEMENTS**

Support of the National Science Foundation under Grant Nos. INT-86-17683 and PHY-86-11210, of the Hungarian Academy of Sciences, and of the Conselho Nacional de Desenvolvimento Cientifico e Tecnologico, Brazil, is gratefully acknowledged.

ϕ Present address: UVSOR, Institute for Molecular Science, Okazaki, Japan
† Present address: Lawrence Berkeley Laboratory, Berkeley, CA 94720
* Present address: Lawrence Livermore Nuclear Laboratory, Livermore, CA 94550
α Present address: Ohio University, Athens, OH 45701

**REFERENCES**

1. D. BOHNE, C. WUZHONG and M. MULLER; R. SPOHR, GSI Nachrichten 12-91, pp. 11-13, December, 1991.
2. R.J.MICHAEL FRY, J.D. BOICE, Jr., V.P. BOND, S.B. CURTIS and D. GRAHN, "Guidance on Radiation Received in Space Activities," NCRP Report No. 98, National Council on Radiation Protection and Measurements, Bethesda, Md., July 31, 1989.
3. R. MADEY, W.-M. ZHANG, A.R. BALDWIN, M. ELASSER, B.S. FLANDERS, D. KEANE, W. PAIRSUWAN, J. VARGA, J.W. WATSON, G.D. WESTFALL, C. HARTNACK, H. STÖCKER, and K. FRANKEL, Phys. Rev. C 42, 1068 (1990).
4. R. MADEY, W.-M. ZHANG, B.D. ANDERSON, A.R BALDWIN, B.S. FLANDERS, W. PAIRSUWAN, J. VARGA, J.W. WATSON, and G.D. Westfall, Phys. Rev.C 38, 184 (1988).
5. R.A. CECIL, B.D. ANDERSON, A.R. BALDWIN, R. MADEY, A. GALONSKY, P. MILLER, L. YOUNG and F.M. WATERMAN, Phys. Rev. C 21, 2471 (1980).
6. H.R. SCHELIN, A. GALONSKY, C.K. GELBKE, L. HEILBRONN, W.G. LYNCH, T. MURAKAMI, M.B. TSANG, X. YANG, G. ZHANG, B.A. REMINGTON, F. DEAK, A. KISS, Z. SERES and J. KASAGI, Phys. Rev. C **39**, 1827 (1989).
7. D. SACKETT, A. GALONSKY, C. K. GELBKE, H. HAMA, L. HEILBRONN, D. KROFCHECK, W. LYNCH, H.R. SCHELIN, M.B. TSANG, X. YANG, F. DEAK, A. HORVATH, A. KISS, Z. SERES, J. KASAGI and T. MURAKAMI, Phys. Rev. C **44**, 384 (1991).
8. J. HELTSLEY, L. BRANDON, A. GALONSKY, L. HEILBRONN, B.A. REMINGTON, S. LANGER, A. VANDER MOLEN, and J. YURKON, Nucl. Instrum. Methods Phys. Res. A **263**, 441 (1988).
9. R.A. CECIL, B.D. ANDERSON, and R. MADEY, Nucl. Instr. Methods **161**, 439 (1979).
10. T.C. AWES, G. POGGI, S. SAINI, C.K. GELBKE, T. LEGRAIN, and G.D. WESTFALL, Phys. Lett. **103B**, 417 (1981).

**Table I. Moving-source parameter values.** Equation 1 with the parameter values in this table were used for the fits shown by the solid lines in Fig. 1 and for all the curves in Figs. 2 and 3. The first reaction is reported in this paper; the second and third reactions are reported in Refs. 6 and 7, respectively.

| | Source #1 | | | Source #2 | | | Source #3 | | |
|---|---|---|---|---|---|---|---|---|---|
| Reaction | T(MeV) | ε(MeV/nuc) | σ(barn) | T(MeV) | ε(MeV/nuc) | σ(barn) | T(MeV) | ε(MeV/nuc) | σ(barn) |
| $^{14}$N E/A = 50 MeV | 3.7 | 1.7 | 9.2 | 11.4 | 18.1 | 6.3 | 2.04 | 39.3 | 0.61 |
| $^{14}$N E/A = 35 MeV | 4.0 | 0.45 | 12.2 | 11.1 | 12.8 | 2.3 | 2.2 | 30 | 0.71 |
| $^{36}$Ar E/A = 35 MeV | 4.2 | 0.56 | 19.1 | 11.4 | 11.8 | 3.9 | 3.6 | 24.6 | 3.2 |

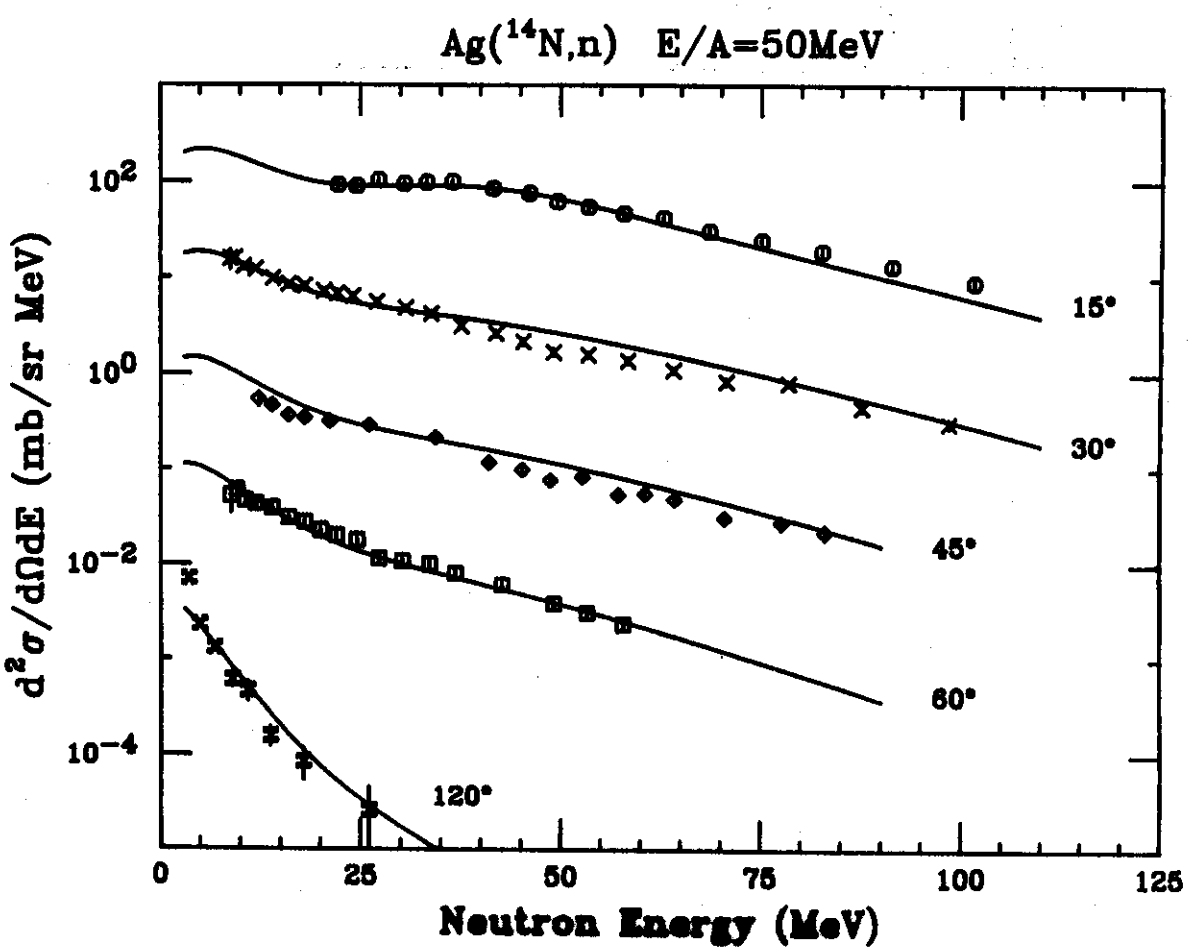


**Fig. 1. Neutron energy spectra at five angles.** The solid lines are the fits using three thermal sources. The vertical scale is correct for the 15° data and curves; for clarity the others have been lowered by successive factors of 10.

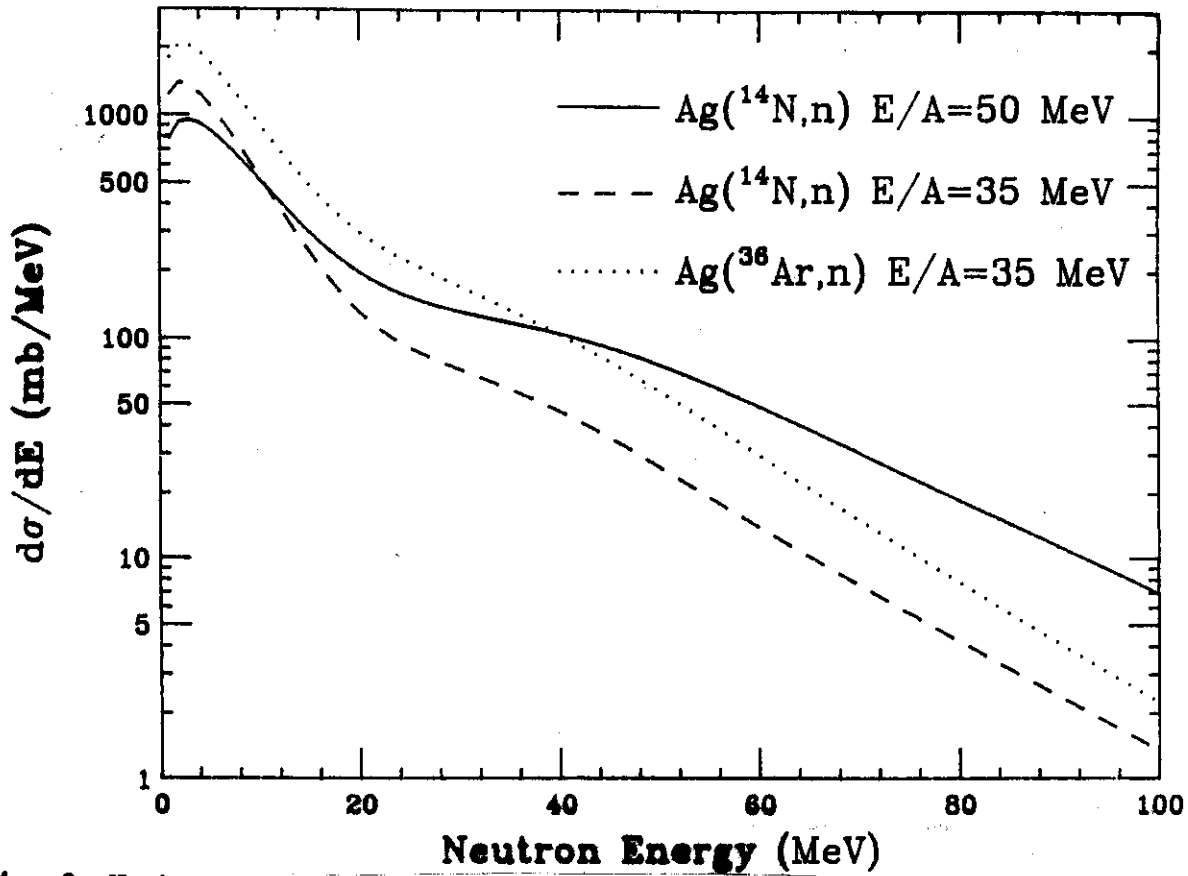


**Fig. 2. Neutron energy spectra integrated over angle.** The solid line corresponds to the reaction $^{14}$N + Ag at E/ A =50 MeV, the dashed line to the reaction $^{14}$N + Ag at E/A = 35 MeV, and the dotted line to the reaction $^{36}$Ar + Ag at E/A = 35 MeV.

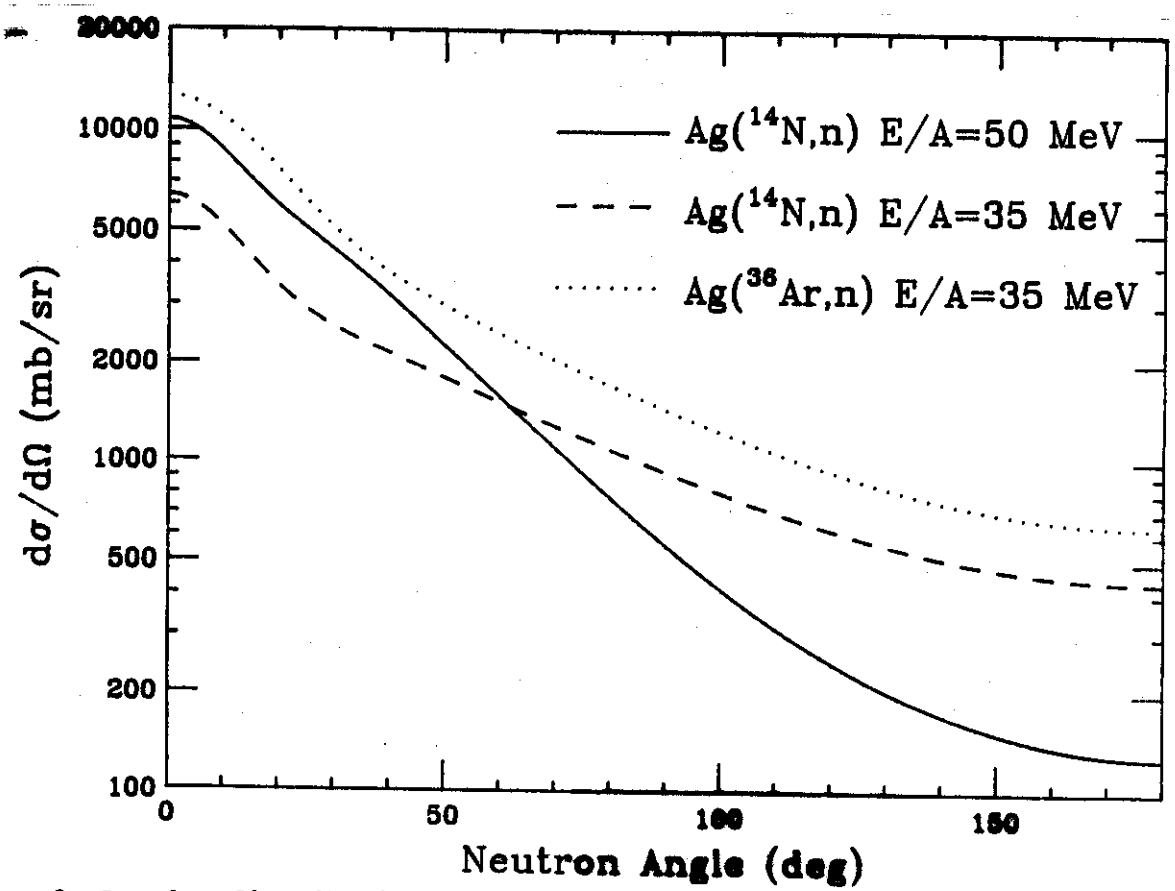


**Fig. 3. Angular distributions integrated over energy.** The solid line corresponds to the reaction $^{14}$N + Ag at E/A = 50 MeV, the dashed line to the reaction $^{14}$N + Ag at E/A = 35 MeV, and the dotted line to the reaction $^{36}$Ar + Ag at E/A = 35 MeV.